 https://doi.org/10.24191/jeesr.v29i1.027

Smart Flood Early Warning System with AI Prediction and LoRa Communication (FloodGuard AI)

Muhamad Akmal Harith Mohd Bakhtiar, Suzi Seroja Sarnin*, Nur Syahirah Saipul, Norlela Ishak, Nani Fadzlina Naim, Mohd Rizal Dohad and Ros Shilawani S Abdul Kadir

***Abstract*—FloodGuard AI is a prototype flood monitoring and risk-classification platform integrating an HC-SR04 ultrasonic water-level sensor, YL-83 rain sensor, Random Forest classifier, SX1262 LoRa communication, solar-battery power, and ESP32-CAM visual monitoring. Unlike a stand-alone threshold alarm, the prototype combines sensor trends with three-class risk inference and returns the classification to a local LED/siren node via a LoRa acknowledgment. Evaluation comprised controlled calibration, indoor link verification, and monitoring records collected between 30 January and 24 June 2026. The water-level sensor achieved 1.6 cm mean absolute error in 30 controlled measurements. The classifier attained 99.0% accuracy on a 200-sample held-out set and 92.9% on 420 valid monitoring records. Indoor bidirectional LoRa testing delivered 93 acknowledgments for 93 packets (100% packet delivery); outdoor 1 km performance was not validated with distance-specific packet delivery measurements. These results demonstrate prototype feasibility, while flood-event validation, independent risk labels, and outdoor link characterization remain necessary before operational deployment.**

***Index Terms*—Flood early warning, Internet of things (IoT), LoRa, random forest, risk classification, solar-powered monitoring.**

I. INTRODUCTION

Malaysia experiences flooding almost every year, and the monsoon seasons usually bring the most severe events. These floods affect both urban and rural areas, damaging homes, roads, and infrastructure, and in the worst cases they cost people their lives [1]. Urban areas tend to struggle with poor drainage and the pressure of rapid development, while rural and remote areas are often left with patchy communication infrastructure, and that gap makes disaster response even slower than it already is [2].

Conventional water-level alarms generally trigger when a predefined threshold is exceeded, limiting their ability to account for concurrent rainfall and changing water-level trends. Communication and power availability are additional constraints for monitoring installations in remote or flood-prone areas. However, these limitations vary by deployment and should not be generalized to all existing systems. The present work therefore evaluates whether low-cost sensing, local LoRa alerts, solar-battery supply, and server-side machine-learning classification can be integrated in one prototype.

FloodGuard AI combines Internet of Things (IoT) sensing, a Random Forest risk classifier, long-range (LoRa) radio, solar-battery power, and visual monitoring. Here, artificial intelligence (AI) refers specifically to supervised machine-learning classification; Global System for Mobile Communications (GSM) is discussed only as a communication approach used by some prior systems, not as part of the proposed LoRa link. Long short-term memory (LSTM) is a recurrent neural-network architecture referenced in related flood-forecasting work. The research contribution is an integrated, bidirectional prototype that returns the server-computed risk label to the field node through the LoRa acknowledgment, alongside a comparison of held-out and monitoring-record classification performance. The study evaluates feasibility, not a verified advance-warning lead time.

Recent work shows sensor driven flood detection is effective in the field. Nik Mohd Kamal et al. built an IoT based flood detection system around a NodeMCU ESP8266, an ultrasonic sensor, and time series forecasting [3]. Yahya and Homam used an ESP32, an ultrasonic sensor, and LoRa to keep monitoring reliably where Wi-Fi or GSM is unavailable [4]. Zakaria et al. developed a LoRaWAN based system that kept power consumption low while still delivering real time alerts [5]. These projects proved sensor based detection is feasible, but most stopped at threshold based alerting rather than prediction. Md Yassin et al. similarly demonstrated a LoRa based system suited to areas with weak network coverage [6].

On the prediction side, the trend has moved toward machine learning. Zhou et al. paired LSTM networks with Bayesian optimization to forecast floods across space and time, reaching high accuracy in urban settings [7]. Widiasari and Efendi used a hybrid LSTM-GRU model for water level prediction with better short term forecasts [8]. Li et al. combined LSTM with hydrological data and outperformed traditional statistical methods [9]. Arante et al. blended fuzzy logic, LSTM, and genetic algorithms to improve reliability and reduce false alarms [10]. These studies make a strong case for prediction, though they assume a continuous data stream that is hard to guarantee in a low cost, off grid deployment. Keerthi Reddy et al. confirmed the advantage of machine learning over

This manuscript is submitted on August 21, 2026, revised on October 19, 2026, accepted on October 20, 2026, and published on October 31, 2026.

All authors are with the Faculty of Electrical Engineering, Universiti Teknologi MARA, Selangor Branch, Shah Alam, Malaysia.

*Corresponding author
Email address: suzis045@uitm.edu.my

1985-5389/© 2026 The Authors. Published by UiTM Press. This is an open access article under the CC BY-NC-ND license (http://creativecommons.org/licenses/by-nc-nd/4.0/).

conventional rule based methods [11].

Beyond ground-based sensing, related studies examine camera-based monitoring and remote sensing. Lee et al. used RGB and thermal imagery for flood monitoring [12], while satellite-based methods have been explored in [13]–[15]. Such approaches address different spatial scales and data requirements from the present low-cost, site-specific sensor node. Additional work by Razavi-Termeh et al. was mentioned in an earlier draft but is omitted here pending verification of its full bibliographic details.

The reviewed literature illustrates complementary approaches rather than a universal deficiency in previous flood-warning systems. FloodGuard AI focuses on the practical integration of four functions within one testable prototype: water-level/rain sensing, three-level classification using water-level trends, bidirectional LoRa feedback for local alerts, and solar-powered monitoring with optional camera inspection. Table I is a qualitative functional comparison, not a systematic survey; individual capabilities of prior systems are discussed in the cited studies [3]–[15].

TABLE I. COMPARISON OF EXISTING SYSTEMS VS. FLOODGUARD AI

Aspect	Existing Systems	FloodGuard AI
Detection	Threshold based	AI classification
Prediction	Reactive only	Low / Medium / High
Communication	Wi-Fi / GSM	LoRa (long range)
Power Supply	Grid / battery	Solar + battery
Visual Check	Not available	ESP32-CAM live feed
Scalability	Limited	Multi node ready

This study investigates whether a prototype can (i) measure water level to within ±2 cm under controlled calibration, (ii) classify Low, Medium, and High risk with at least 80% test accuracy, and (iii) support a LoRa link designed for 1 km range and at least 90% packet delivery. The third target requires fixed-distance outdoor validation and is not established by the present indoor tests.

II. RESEARCH METHODOLOGY

Development followed an iterative sequence: requirements and related-work review, hardware selection and assembly, sensor and software integration, model development, LoRa messaging, and subsystem evaluation (Fig. 1). The available evidence comprises controlled water-level calibration, indoor two-room LoRa packet tests, and sensor records obtained during an outdoor monitoring phase. Although outdoor monitoring is reported, the manuscript does not establish a validated natural-flood deployment or controlled simulation of a real flood event. Photographs of the assembled sensor testbed, its placement, and the indoor LoRa configuration must be inserted before final submission to make the setup reproducible.

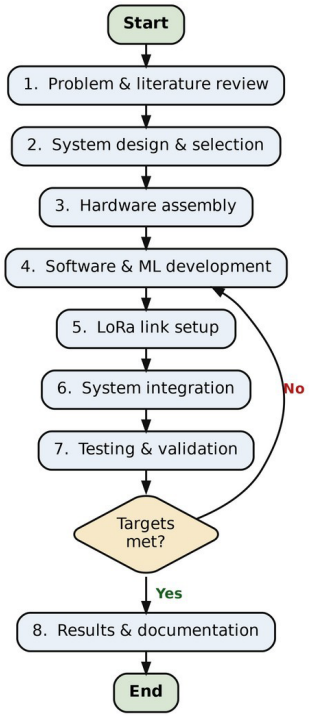


Fig. 1. Development workflow of FloodGuard AI, from problem and literature review through system design, hardware assembly, software and ML development, LoRa link setup, system integration, and testing and validation.

A. System Architecture

FloodGuard AI is arranged as a four layer system. The Sensing Layer relies on the HC-SR04 ultrasonic sensor for water level and the YL-83 rain sensor for rainfall intensity. The Processing and ML Layer uses the Heltec WiFi LoRa 32 V3 to acquire sensor data and handle LoRa transmission, while flood risk inference runs on a Flask server using a scikit-learn Random Forest model. The Communication and Alert Layer carries the built in LoRa SX1262 alongside an active siren for local alerts. The Presentation Layer is a Flask dashboard showing real time sensor data, AI risk status, trends, and ESP32-CAM video. Fig. 2 shows the complete hardware wiring.

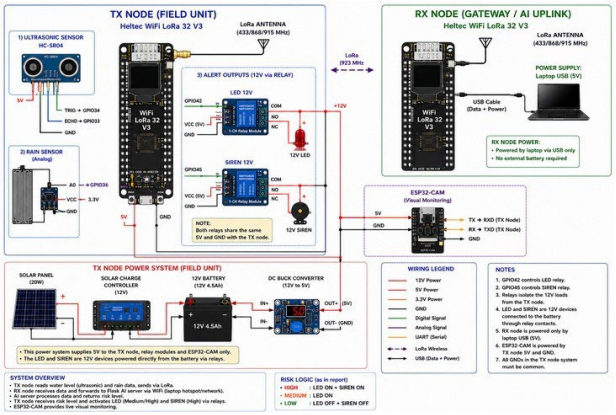


Fig. 2. Complete wiring diagram of the FloodGuard AI TX node (sensors, relays, LED and siren alerts), RX node (LoRa gateway), ESP32-CAM module, and solar power subsystem.

Fig. 3 traces the full operational loop, from how a reading is taken and travels over LoRa to the server, to how the model decides a risk level and that decision drives the alerts and dashboard.

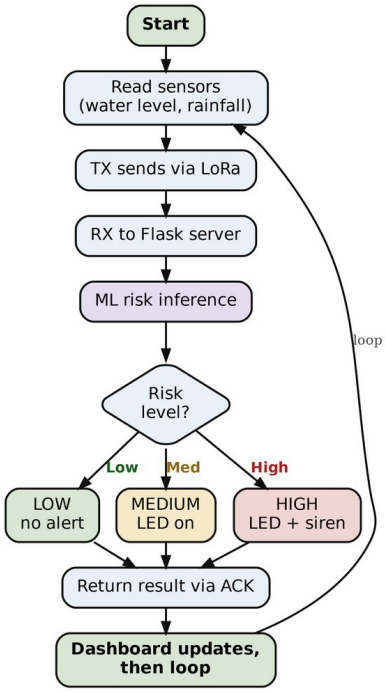


Fig. 3. Overall operational flowchart of FloodGuard AI, from sensor reading and LoRa transmission through server-side ML inference to alert output and dashboard update.

B. AI Based Flood Risk Prediction Model

The AI module uses supervised classification to assign Low, Medium, or High flood-risk categories from water level, rainfall, and rate-of-change features. It is a risk-state classifier rather than a model with a demonstrated forecast horizon. Sensor measurements are sent to the receiver and forwarded to a Flask server for inference; the predicted label is returned to the field node.

A Random Forest was selected as a suitable baseline for the available tabular features. The manuscript reports 1,000 labeled samples, comprising approximately 300 records attributed to historical Department of Irrigation and Drainage Malaysia data and 700 synthetic samples. The stated labels were generated using predefined hydrological rules; consequently, agreement with these labels does not independently establish predictive validity for actual flood outcomes. The precise DID source, sampling method, thresholds, class distribution, and prevention of overlap between training and evaluation records must be documented to enable replication. No verified external citation [17] is available, so the earlier unsupported citation has been removed.

The best configuration was n_estimators = 200, max_depth = 8, min_samples_leaf = 2, and max_features = 0.6. The trained model was saved with joblib and loaded into the Flask server. In operation, the TX node sends raw values over LoRa to the RX gateway, which forwards them to the server by HTTP POST. The server returns the risk classification, relayed back to the TX node inside the LoRa ACK packet so the field node can act locally.

Labels were assigned using predefined rules based on water level, rainfall, and their rates of change. The reported 80/20 stratified split and five-fold cross-validation apply to the model-development dataset. The 420 valid monitoring records were evaluated separately; however, independence from rule-generated labels and the occurrence of actual flood events have not been established. The 99.0% held-out accuracy should therefore be interpreted as performance against the study labels, not as proven real-world flood prediction accuracy.

C. Hardware Components

Table II lists the main hardware and software pieces that make up the FloodGuard AI system.

TABLE II. FLOODGUARD AI HARDWARE AND SOFTWARE COMPONENTS

Component	Model	Function
Ultrasonic Sensor	HC-SR04	Water level measurement (±2 cm)
Rain Sensor	YL-83	Rainfall intensity, fast response
Microcontroller	Heltec WiFi LoRa 32 V3	Data acquisition and control
Camera Module	ESP32-CAM	Visual monitoring, Wi-Fi streaming
LoRa	SX1262 (built in)	Long range transmission
AI Framework	Scikit-learn	Flood risk prediction
Web Platform	Flask	Real time data visualisation
Power Supply	Solar + 12V 4.5Ah SLA	Autonomous operation
Alert System	Siren + LED	Local warning, no internet needed

D. System Operation

The transmitter (TX) samples water level and rainfall and sends measurements over LoRa to a receiver (RX), which forwards them to a Flask server for classification. The predicted class is returned through the LoRa acknowledgment to control the local LED and siren (Fig. 3). This architecture requires the RX-to-server processing path for model-based decisions; therefore, an uninterrupted internet-independent inference capability has not been demonstrated. Any fail-safe local threshold rule, offline inference, or cached classification should be explicitly implemented and tested before claiming continued alerts during gateway/server outages.

E. System Testing and Validation

Validation consisted of five categories: controlled water-level calibration against ruler measurements; classification on held-out and monitoring records; indoor LoRa packet delivery and received-signal measurements; end-to-end dashboard and alert response; and solar-battery operation. Indoor two-room testing was necessary to verify packet/acknowledgment handling and local alarm actuation before outdoor use; it does not establish outdoor range. The sensor testbed configuration (sensor mounting height, reference scale, water container or monitoring site, sensor protection, and collection intervals) and photographs of the actual setup remain required for reproducibility. No distance-specific outdoor packet delivery rate (PDR) or received signal strength indicator (RSSI) dataset

is available in the manuscript.

III. Results and Discussion

The following subsections report the controlled sensor calibration, classifier results, indoor LoRa communication, system integration, and power observations. Table III summarizes the objective-level outcomes to distinguish measured outcomes from unverified targets.

TABLE III. Summary of Results Against Objectives

Objective	Target	Result	Status
1 Sensing	±2 cm level accuracy	1.6 cm MAE	Met
2 AI prediction	≥80% accuracy	99.0% / 92.9%	Met
3 LoRa link	≥1 km, ≥90% PDR	100% PDR (indoor), ~1 km (preliminary)	Partially Met

A. Sensor Calibration and Accuracy

From 30 January to 24 June 2026, the system recorded 509 raw ultrasonic readings, of which 89 (17.5%) were invalid (-1), leaving 420 valid records for analysis. The invalid values were attributed to missing echoes, possible turbulence, sensor startup, or beam obstruction. The firmware flagged invalid readings; however, the present evidence does not document a tested fail-safe response to consecutive invalid measurements. A future safety-oriented implementation should retain the last valid reading only for a bounded interval, raise a sensor-fault warning after repeated timeouts, and avoid interpreting -1 as a safe water level. These safeguards require firmware verification and fault-injection testing.

Accuracy was checked against a ruler based reference at 20 cm, 60 cm, and 100 cm. The MAE across 30 calibration measurements came out at 1.6 cm, inside the ±2 cm target set in Objective 1. Across 149 stable deployment readings the mean deviation was 2.1 cm with a maximum of 9.8 cm, reflecting real surface turbulence rather than any hardware fault. The ±2 cm target was therefore achieved during controlled calibration, while outdoor deployment showed higher deviation.

Fig. 4 plots the water level trend across the full monitoring period, with background shading marking the risk zone assigned by the ML classifier. The shaded bands confirm that the High-Risk readings line up with the moments when the water level climbed sharply.

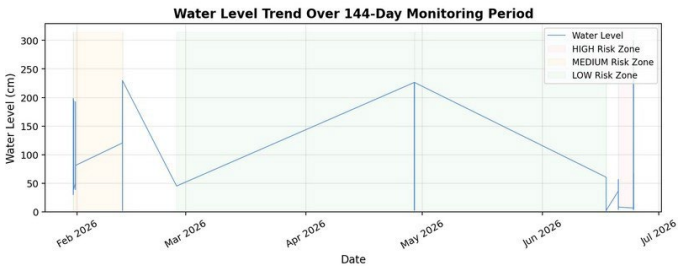


Fig. 4. Water level trend across the 144 day monitoring period (30 January to 24 June 2026), with background shading showing the ML classified risk zones.

B. AI Model Performance

On the held out test set of 200 samples, the classifier reached an overall accuracy of 99.0% and a ROC-AUC of 0.9999, well above the 80% target in Objective 2. As Table IV shows, precision, recall, and F1-score all stayed high across the three classes.

TABLE IV. Classification Report on Test Set (n = 200)

Class	Precision	Recall	F1-score
High	1.00	1.00	1.00
Medium	0.99	0.99	0.99
Low	0.98	0.98	0.98
Accuracy	-	-	0.99
Macro avg	0.99	0.99	0.99

Fig. 5 shows the confusion matrix. Out of 200 samples only two were misclassified, both slipping between the Low and Medium classes. Every one of the 67 High Risk samples was classified correctly, which counts for a lot in a flood warning setting, since a missed High Risk detection could be the difference in getting people out in time.

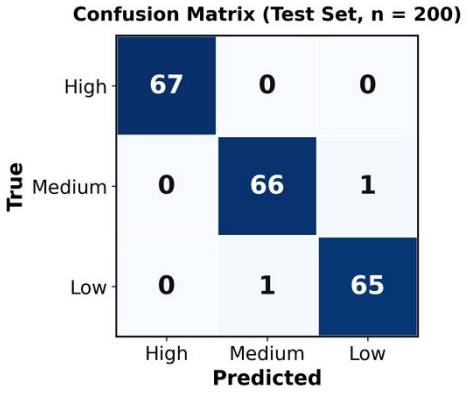


Fig. 5. Confusion matrix of the Random Forest flood risk classifier on the test set.

Fig. 6 breaks down the importance of features. The current water level was by far the most influential at 58.3%, followed by the rate of change in water level at 25.2%, with rainfall rate at 12.4% and cumulative rainfall at 4.1%. That ordering lines up with flood physics, where a rapidly rising water level is the clearest sign of imminent risk while rainfall plays a supporting role.

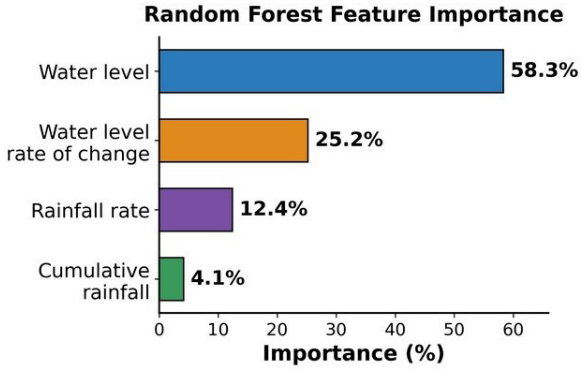


Fig. 6. Feature importance ranking from the Random Forest flood risk classifier.

A simple water-level/rainfall threshold baseline (water level above 150 cm or rainfall above 40 mm) reportedly achieved approximately 82% accuracy, compared with 99.0% for the Random Forest on the held-out dataset. This is a difference of approximately 17 percentage points under the study labeling protocol. Because the risk labels were derived from predefined rules, the comparison must not be interpreted as independent proof of superior flood forecasting. On 420 valid monitoring records, reported accuracy was 92.9% and macro F1-score was 0.92; the original evaluation reported no missed High Risk labels. Event-level validation against independently verified flood outcomes remains outstanding.

The lower accuracy on monitoring records (92.9%) relative to the held-out dataset (99.0%) is consistent with possible measurement variation, but the causes have not been experimentally isolated. The classifier emphasizes water level and its rate of change, as shown in Fig. 6. Without an independently verified flood-event reference and measured warning lead time, the findings support risk-label classification performance only, not a demonstrated ability to predict flood onset in advance.

C. *LoRa Communication Range and Reliability*

The LoRa link was tested with two Heltec WiFi LoRa 32 V3 boards, one as the TX node and one as the RX node, both running the built in SX1262 transceiver. A custom ACK handshake protocol was implemented so that after the TX node sends its sensor data, the RX node replies with the ML risk level, confirming delivery and sharing the risk classification in a single exchange.

During indoor testing across two rooms, the system completed full bidirectional exchanges without trouble. The RX node picked up packets at an RSSI of around -114 dBm with an SNR between -9 and -11 dB. With the SX1262 sensitivity floor near -148 dBm, that leaves a link margin of roughly 34 dB, comfortable indoors but quickly eaten up outdoors. In all, 93 uplink packets were sent and 93 ACK replies came back, giving 100% packet delivery indoors. Of those, 31 were High Risk and switched on both the LED (GPIO42) and the siren (GPIO45), following the alert logic in Table V.

TABLE V. ALERT OUTPUT LOGIC BY RISK LEVEL

Risk Level	LED (GPIO42)	Siren (GPIO45)
Low	Off	Off
Medium	On	Off
High	On	On

The TX node also carried a retry mechanism. Whenever the RX node did not reply, the TX node automatically retried up to three times before moving on, which trimmed packet loss without manual intervention. The firmware also flagged bad sensor readings with a warning message, which is why some entries ended up stored as -1 in the dataset. This combination of retries and error handling kept the system running steadily throughout the tests.

Outdoor communication at approximately 1 km was discussed as a preliminary target, but the distance-dependent PDR and RSSI values shown in Fig. 7 are generated from an estimated propagation model using measured indoor RSSI, free-space path loss, and an assumed obstruction penalty. They are not measured outdoor results. Consequently, the 1 km / ≥90% PDR objective remains unverified. A subsequent field campaign should report transmitter/receiver antenna heights, line of sight, transmit power, spreading factor, bandwidth, coding rate, packet count, PDR, RSSI, and SNR at fixed distances such as 200, 500, and 1,000 m. Fig. 7 must remain explicitly labeled "estimated" and must not be cited as empirical range validation.

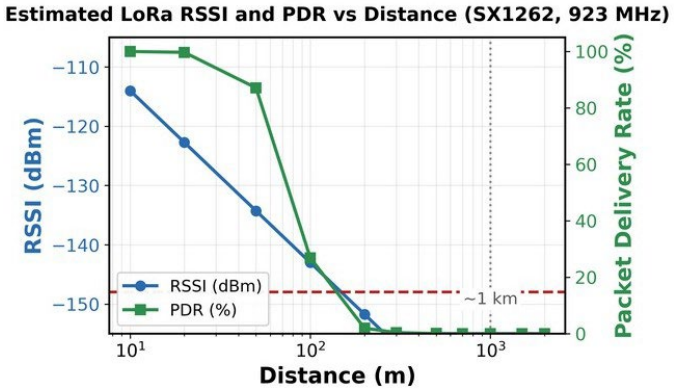


Fig. 7. Estimated LoRa RSSI and Packet Delivery Rate (PDR) versus distance for the SX1262 at 923 MHz, based on the measured indoor RSSI of -114 dBm.

D. *System Integration and Alert Response*

The reported monitoring period ran from 30 January to 24 June 2026 and included indoor verification and outdoor monitoring. The manuscript describes 13 indoor and 118 outdoor days, which total 131 rather than 144 days; the remaining 13 days and the exact phase boundaries require reconciliation from the original logs. The Flask dashboard displayed received measurements and classification results, with reported median update intervals of 3.0 s indoors and 6.0 s outdoors. These observations demonstrate prototype integration, not a validated real-flood warning trial.

Fig. 8 captures the dashboard during a live Medium Risk event on 24 June 2026, with a water level of 37.9 cm, rainfall of 22.8 mm, and 30 °C under Rainy weather. It correctly showed Medium risk alongside the ML output and the recent water level trend, while the readings table and ESP32-CAM feed confirmed that multi sensor logging and visual monitoring worked together as one platform, without manual control or internet for the core alert functions.



Fig. 8. FloodGuard AI web dashboard showing live sensor readings, ML based risk classification, and the water level trend

during a Medium Risk event (24 June 2026).

Fig. 9 shows the recent readings table and the ESP32-CAM panel. The table lists the last few readings with their timestamp, water level, rainfall, temperature, weather, and AI risk label, and that label switches correctly between High, Medium, and Low as the values move. The ESP32-CAM panel carries the live feed, so conditions can be confirmed visually without travelling to the site.

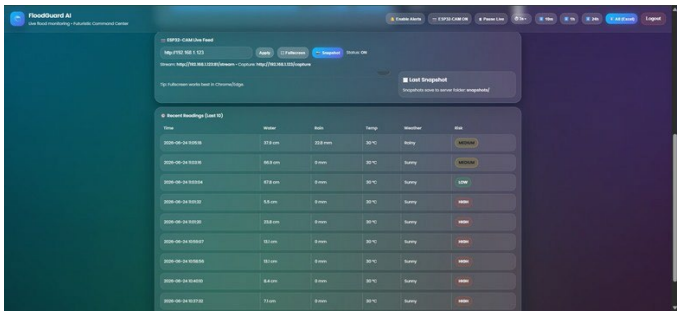


Fig. 9. FloodGuard AI recent readings table and ESP32-CAM live feed panel, confirming multi sensor data logging and visual monitoring in one interface.

E. Power System Performance

The prototype used a 12 V solar panel, charge controller, and 12 V, 4.5 Ah sealed lead-acid battery (nominal energy 54 Wh), with regulated power for the Heltec board and ESP32-CAM. The reported nominal load of approximately 350 mA at 12 V suggests a theoretical energy-to-load ratio of approximately 12.9 h, excluding discharge limits and conversion losses; actual autonomy was not measured through a controlled battery discharge test. Battery voltage monitoring was absent. A calibrated resistor-divider circuit connected to a suitable analog input, with appropriate overvoltage protection and ADC calibration, could support low-voltage alerts and future state-of-charge estimation.

F. Overall System Evaluation

The controlled calibration target was achieved (1.6 cm MAE), whereas outdoor deviations were higher. Classification achieved the reported 99.0% held-out and 92.9% monitoring-record accuracy, subject to limitations of rule-derived labels and absent independently verified flood events. Indoor LoRa delivery was 93/93 packets; the 1 km outdoor PDR target was not validated. The integrated prototype also demonstrated dashboard display and local alarm actuation under the tested conditions. Full outdoor communications characterization, failure-mode testing, and natural-event validation are required before operational deployment.

The results also show the design behaves as one connected system rather than a set of parts tested in isolation. The sensors feed the model, the result travels back to the field node over LoRa, the alerts fire locally, and the dashboard mirrors everything for a remote user. Because low cost sensors and open source tools kept the build affordable, the same design could be copied across several nodes reporting into one dashboard.

IV. CONCLUSION

This paper presented the design, development, and testing of FloodGuard AI, a smart flood early warning system that leans on IoT sensors, AI prediction, and LoRa communication to monitor floods autonomously. It was built to answer the main weaknesses of the approaches already used in Malaysia: reliance on internet connectivity, lack of predictive capability, limited communication range, and the absence of visual monitoring.

The prototype achieved 1.6 cm controlled calibration MAE, 99.0% held-out classification accuracy, 92.9% accuracy on valid monitoring records, and 100% indoor acknowledgment delivery (93/93 packets). These results support the feasibility of combining low-cost sensing, LoRa messaging, solar-battery power, server-side risk classification, and visual monitoring. They do not establish a verified 1 km outdoor communication link, an independently measured flood-warning lead time, or reliable operation during actual flood emergencies. Further work should include fixed-distance outdoor PDR/RSSI tests, photographs and full description of the testbed, independently labeled flood-event datasets, sensor-fault handling, server-outage fail-safe testing, battery-voltage monitoring, and privacy-aware camera deployment.

ACKNOWLEDGMENT

The authors would convey their profound appreciation and gratitude to the Faculty of Engineering, Universiti Teknologi MARA, Shah Alam, Selangor, Malaysia for permitting us to perform this study. Special thanks to those who contributed to this project directly and indirectly.

REFERENCES

[1] Department of Irrigation and Drainage Malaysia, "Annual flood report Malaysia 2023," DID Malaysia, Kuala Lumpur, Malaysia, 2023.

[2] World Meteorological Organization, "Guidelines on multi-hazard early warning systems," WMO Publications, Geneva, Switzerland, 2021.

[3] N. N. M. S. Nik Mohd Kamal, A. A. Zainuddin, A. U. Shamsudin, M. S. Sapuan, M. H. A. Samsudin, and M. A. H. Zulkfli, "Development and implementation of an IoT-based early flood detection and monitoring system utilizing time series forecasting for real-time alerts in resource-constrained environments," *Malaysian J. Sci. Adv. Technol.*, vol. 5, no. 1, pp. 30–36, Jan. 2025, doi: 10.56532/mjsat.v5i1.370.

[4] N. L. Yahya and M. J. Homam, "Real-time flood monitoring alert system with LoRa and IoT," *Evol. Elect. Electron. Eng.*, vol. 6, no. 1, pp. 92–102, 2025, doi: 10.30880/eeee.2025.06.01.013.

[5] M. I. Zakaria, W. A. Jabbar, and N. Sulaiman, "Development of a smart sensing unit for LoRaWAN-based IoT flood monitoring and warning system in catchment areas," *Internet Things Cyber-Phys. Syst.*, vol. 3, pp. 249–261, 2023, doi: 10.1016/j.iotcps.2023.04.005.

[6] M. I. H. Md Yassin, T. W. Au, S. H. Shah Newaz, and S. Omar, "LoRa-based real-time flood detection and monitoring system: A Brunei Darussalam-based study," in *Proc. Int. Conf. Electron., Commun. Inf. Technol. (ICECIT)*, 2021, pp. 1–5, doi: 10.1109/ICECIT54077.2021.9641097.

[7] Q. Zhou *et al.*, "A deep-learning-technique-based data-driven model for accurate and rapid flood predictions in temporal and spatial dimensions," *Hydrol. Earth Syst. Sci.*, vol. 27, no. 9, pp. 1791–1808, May 2023, doi: 10.5194/hess-27-1791-2023.

[8] I. R. Widiasari and R. Efendi, "Utilizing LSTM-GRU for IoT-based water level prediction using multi-variable rainfall time series data," *Informatics*, vol. 11, no. 4, Art. no. 73, Oct. 2024, doi: 10.3390/informatics11040073.

[9] J. Li, G. Wu, Y. Zhang, and W. Shi, "Optimizing flood predictions by integrating LSTM and physical-based models with mixed historical and

simulated data," *Heliyon*, vol. 10, no. 13, Art. no. e33669, 2024, doi: 10.1016/j.heliyon.2024.e33669.

[10] H. R. C. Arante, E. Sybingco, M. A. Roque, L. Ambata, A. Chua, and A. N. Gutierrez, "Development of a secured IoT-based flood monitoring and forecasting system using genetic-algorithm-based neuro-fuzzy network," *Sensors*, vol. 25, no. 13, Art. no. 3885, Jun. 2025, doi: 10.3390/s25133885.

[11] D. Keerthi Reddy, "Flood prediction using machine learning," *Int. J. Multidiscip. Res. Sci. Eng. Technol. Manage. (IJMRSETM)*, vol. 10, no. 5, 2023.

[12] Y. J. Lee, J. Y. Hwang, J. Park, H. G. Jung, and J. K. Suhr, "Deep neural network-based flood monitoring system fusing RGB and LWIR cameras for embedded IoT edge devices," *Remote Sens.*, vol. 16, no. 13, Art. no. 2358, Jun. 2024, doi: 10.3390/rs16132358.

[13] B. Ghosh, S. Garg, and M. Motagh, "Automatic flood detection from Sentinel-1 data using deep learning architectures," *ISPRS Ann. Photogramm. Remote Sens. Spatial Inf. Sci.*, vol. V-3-2022, pp. 201–208, 2022, doi: 10.5194/isprs-annals-V-3-2022-201-2022.

[14] B. Shahi, A. Poudel, A. Dahal, and S. Upadhyaya, "Flood hazard modelling assessment using deep learning and Earth observation," *J. Geoinformatics, Nepal*, vol. 24, no. 1, pp. 41–47, May 2025, doi: 10.3126/njg.v24i1.79347.

[15] Y. Awasthi and J. Chinzvende, "Deep learning-based flood forecasting using satellite imagery and IoT sensor fusion," *Int. J. Comput. Appl.*, vol. 187, no. 21, pp. 37–42, Jul. 2025, doi: 10.5120/ijca2025925261.